Comparative analyses of plasma probe diagnostics techniques

V. A. Godyak and B. M. Alexandrovich

Citation: Journal of Applied Physics **118**, 233302 (2015); doi: 10.1063/1.4937446
View online: http://dx.doi.org/10.1063/1.4937446
View Table of Contents: http://scitation.aip.org/content/aip/journal/jap/118/23?ver=pdfcov
Published by the AIP Publishing

Comparative analyses of plasma probe diagnostics techniques

V. A. Godyak[1] and B. M. Alexandrovich[2]
[1]*Electrical Engineering and Computer Science Department, University of Michigan, Ann Arbor, Michigan 48109, USA and RF Plasma Consulting, Brookline, Massachusetts 02446, USA*
[2]*Plasma Sensors, Brookline, Massachusetts 02446, USA*

(Received 3 August 2015; accepted 26 November 2015; published online 15 December 2015)

The subject of this paper is a comparative analysis of the plasma parameters inferred from the classical Langmuir probe procedure, from different theories of the ion current to the probe, and from measured electron energy distribution function (EEDF) obtained by double differentiation of the probe characteristic. We concluded that the plasma parameters inferred from the classical Langmuir procedure can be subjected to significant inaccuracy due to the non-Maxwellian EEDF, uncertainty of locating the plasma potential, and the arbitrariness of the ion current approximation. The plasma densities derived from the ion part of the probe characteristics diverge by as much as an order of magnitude from the density calculated according to Langmuir procedure or calculated as corresponding integral of the measured EEDF. The electron temperature extracted from the ion part is always subjected to uncertainty. Such inaccuracy is attributed to modification of the EEDF for fast electrons due to inelastic electron collisions, and to deficiencies in the existing ion current theories; i.e., unrealistic assumptions about Maxwellian EEDFs, underestimation of the ion collisions and the ion ambipolar drift, and discounting deformation of the one-dimensional structure of the region perturbed by the probe. We concluded that EEDF measurement is the single reliable probe diagnostics for the basic research and industrial applications of highly non-equilibrium gas discharge plasmas. Examples of EEDF measurements point up importance of examining the probe current derivatives in real time and reiterate significance of the equipment technical characteristics, such as high energy resolution and wide dynamic range.
[http://dx.doi.org/10.1063/1.4937446]

I. INTRODUCTION

The electrical probe (Langmuir probe) introduced by Langmuir[1] has been the major plasma diagnostics tool for a century. It was mostly by means of the electrical probe and the plasma spectroscopy that contemporary knowledge of the gas discharge plasmas has been achieved. Langmuir probes have also been extensively used for diagnostics in industrial plasma devices operated at relatively low gas pressure. Basics of the electrical probe technique covering various aspects of Langmuir probes, including measurement of the electron energy distribution function (EEDF), are given in Refs. 2–10.

A probe immersed in the plasma inevitably causes local plasma disturbance creating sheath and presheath area around the probe, nevertheless, undistorted by the probe plasma parameters can be inferred from the probe I/V, since the local plasma perturbations are accounted within applicability of the Langmuir probe theory. Generally, a probe has to be made small enough for discounting perturbations of the plasma ionization, the electron energy balances, and discharge current redistribution.[7,9]

Simplicity of the Langmuir probe concept creates perception of the probe measurement being a straightforward and predictable procedure. In fact, "There is no plasma diagnostics method other than probe diagnostics where the danger of incorrect measurements and erroneous interpretation of results are so great."[11] This notion made half a century ago fits well to diagnostics of modern-day complex plasmas calling for further refinement of the probe measurement techniques.

The commonly used probe techniques are the classical Langmuir method, assortment of methods utilizing the ion part of the probe characteristic (IPPC), and measurements of the electron energy distribution. These techniques differ in complexity, as well as in capability to reveal detailed and accurate information about the plasma.

The presented article considers three probe diagnostics methods: (a) the classic Langmuir procedure where the plasma density and the electron temperature are inferred from the electron part of the probe characteristic (EPPC), (b) the probe diagnostics based on the ion part of the probe characteristic analyzed according to various theories of orbital and radial ion motion around the probe, and (c) the probe diagnostics of EEDF according to Druyvesteyn formulation. In this article, we not deliberate the basics of these methods assuming reader's awareness of them from numerous textbooks and reviews. We limit our analysis to ubiquitous cylindrical probes in circumstances consistent with existing collisionless probe theories, i.e., the Langmuir-Druyvesteyn theory for electrons and the well-known radial and orbital motion theories for ions. Methods of probe diagnostics in collisional, anisotropic, and magnetized plasmas are described in Refs. 8 and 9.

II. CLASSIC LANGMUIR PROBE

The starting point of the Langmuir probe method is acquisition of the volt/ampere (probe) characteristic, $I_p(V)$, of a small electrode (probe) immersed into the plasma. In accordance

with Langmuir probe theory, the local plasma parameters, i.e., the electron temperature T_e and the plasma density n, can be inferred from the probe characteristic, $I_p(V)$. The probe I/V characteristic is given by the sum of the electron and ion components

$$I_p(V) = I_{e0}\exp(eV/T_e) - I_i(V),$$

where I_p is the probe current, I_{e0} is the electron current to the probe at the plasma potential (at $V = V_s = 0$), $I_{e0} = enS_p(T_e/2\pi m)^{1/2}$ is the electron saturation current, e and m are, correspondingly, the electron charge and mass, T_e is the electron temperature in the units of energy, (eV), S_p is the probe collecting area, I_i is the ion current on the probe, and V is the probe potential referenced to the plasma potential.

An exemplary probe characteristic $I_p(V)$ is shown in Fig. 1(a). The probe characteristic consists of three zones: the ion attracting part at $V < V_f$, the electron repelling part at $V < V_s$, and the electron attracting or electron saturation part at $V > V_s$. Here, V_f is the floating potential. Each part of the $I_p(V)$ carries some information about the plasma parameters; however, obtainability and accuracy of inference of the plasma parameters from different parts of the probe characteristic are substantially different.

Let us start by discussing the classical Langmuir procedure for obtaining the plasma parameters (T_e and n) from the electron repelling part of the probe characteristic. This procedure is valid only for Maxwellian electron energy distribution and absence of electron collisions in the probe vicinity. A detailed list of assumptions and limitations for applicability of the classical Langmuir probe diagnostics is given in Refs. 7–9.

The classical procedure usually starts by extrapolating of the ion current $I_i(V)$ from some high negative potential (where the probe electron current is negligible) to the unidentified yet plasma potential. Fortunately, the plasma parameters inferred with the Langmuir probe procedure are not sensitive to the accuracy of the ion current extrapolation (since at $V > V_f$, $I_i \ll I_e$), and linear extrapolation of $I_i(V)$ is sufficient for obtaining the electron part of the probe characteristic $I_e(V) = I_p(V) - I_i(V)$ at $V > V_f$. On the other hand, at $V < V_f$, $I_e(V)$ obtained from such ion current extrapolation comes out uncertain because the ion extrapolation impact becomes critical. This issue is discussed later in the paper.

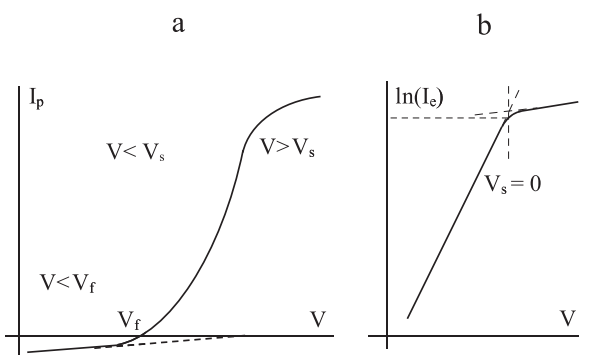

FIG. 1. Ideal probe characteristics in linear (a) and semi-log (b) scale according to the Langmuir concept.

A typical plot of $\ln[I_e(V)]$ shown in Fig. 1(b) is presented in many textbooks and review papers. The linear segment of the $\ln[I_e(V)]$ defines the electron temperature T_e, and the asymptotic crossing point defines the plasma potential, $V = V_s$, and the electron saturation current $I_{e0} = I_e(V = V_s)$. Then, the electron temperature T_e and the plasma density n are found according to well-known formulae

$$T_e = \{d\ln[I_e(V)]/dV\}^{-1} \quad \text{and} \quad n = I_{e0}[eS_p(T_e/2\pi m)^{1/2}]^{-1}.$$

However, in practice, for properly designed probes, there is no clearly displayed saturation of the electron current at $V > V_s$, and a distinctive brake point on the $\ln[I_e(V)]$ curve; the transition from the electron repelling to the electron attracting area is relatively smooth. An experimental probe characteristic look like one shown in Fig. 1 only when the probe is large or/and the plasma density is high, so that the probe sheath thickness is small comparing to the probe radius.

The desire to obtain textbook-like probe characteristics with a visible saturation and a sharp bend leads some beginners to use excessively large probes. Such probes create the plasma disturbances which are difficult to account for and also may cause the voltage applied to the probe to split between the probe sheath and others elements of the probe circuit, resulting in significant inaccuracy of inferred plasma parameters.[9]

The plasma potential found by differentiation $I_p(V)$ gives precise V_s value corresponding to the maximum of dI_p/dV or $d^2I_p/dV^2 = 0$.[7] This is a straightforward and dependable way to find the plasma potential, which is more convenient and often more accurate than that of emissive probe.[6] Attempts to pinpointing the plasma potential directly on the $I_p(V)$ curve create uncertainty due to smooth transition of the probe current to saturation and lead to significant errors in the plasma density inference from the probe characteristic. This is illustrated in Fig. 2 for the probe characteristics and their first derivatives measured in the CCP at 13.56 MHz in the benchmark argon gas at 0.03 and 0.3 Torr.[10]

As seen in Figs. 2(a) and 2(b), there is no distinct bend of the probe characteristics at the true plasma potential located at maximum of dI_p/dV. Presentation of the EPPCs in a semi-log scale $\ln[I_e(V)]$ shown in Fig. 3 allows to find the plasma potential V_{sL} in accordance with the Langmuir procedure (at the point of the asymptotic crossing). The plasma potential for $p = 0.03$ Torr found this way is somewhat higher than the true plasma potential, V_s, found at $d^2I_e(V)/dV^2 = 0$. According to Fig. 3 (and that is typical for plasmas having a Maxwellian distribution for low energy electrons) at 0.03 Torr, the true plasma potential, V_s, falls closer to the inflection point V_{si}, rather than to the asymptotic crossing point V_{sL}.

Much larger error in determining the plasma potential occurs at $p = 0.3$ Torr. In this case, the value of V_{sL} is noticeably lower than the true plasma potential, V_s, found at $d^2I_e(V)/dV^2 = 0$, while at the inflection point, V_{si} is even further from V_s. Such wide gap in determining the plasma potentials lead to an order of magnitude error in finding the

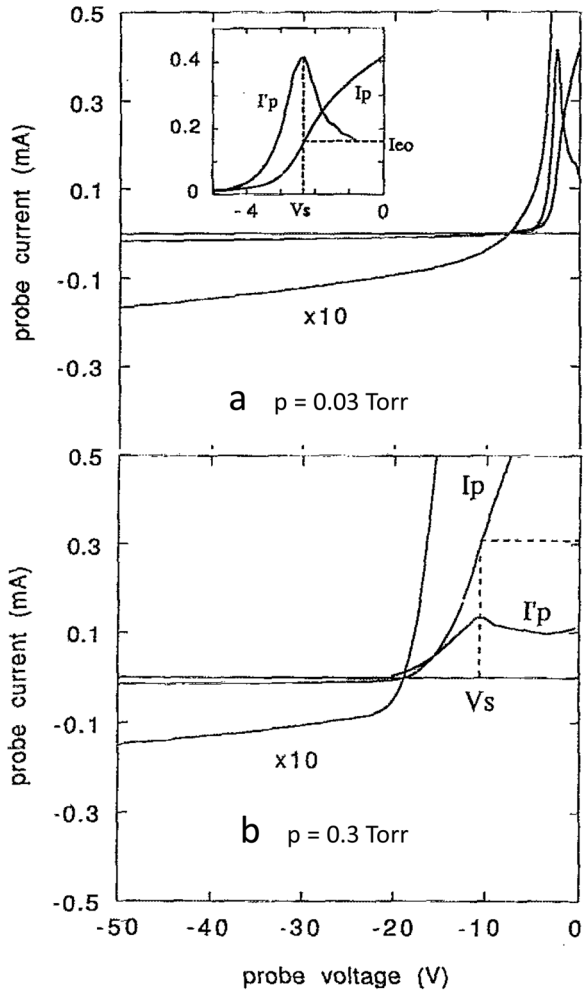

FIG. 2. Probe characteristics $I_p(V)$ and their first derivatives $I'_p(V)$ measured in argon CCP.[10]

electron saturation currents I_{e0} and, correspondingly, in the calculated plasma density. It also worth noting that $I_p(V)$ in the electron saturation area is not an exponent, and the slope

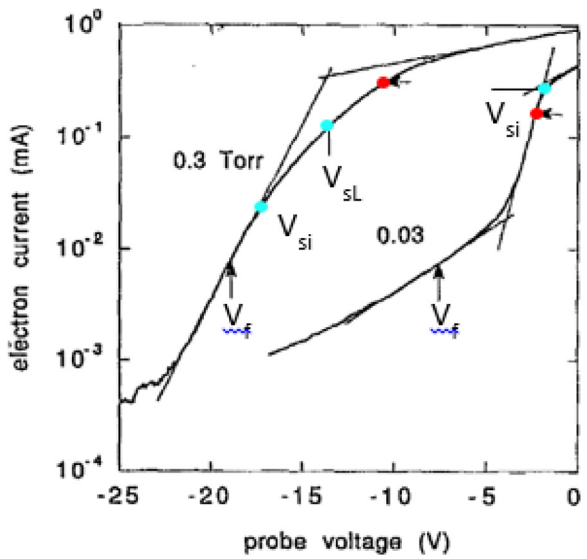

FIG. 3. EEPFs presented in semi-log scale.[10] Horizontal arrows point to the true plasma potentials, V_s found at $d^2I_p/dV^2 = 0$, while vertical arrows point to the floating probe potentials. Also shown here are V_{sL} and V_{si}.

of the line interpolating $\ln[I_e(V)]$ would depend on applied voltage span going beyond the plasma potential, which adds uncertainty to finding the potential V_{sL} at the asymptotic crossing point.

The case of $p = 0.03$ Torr shown in Fig. 3 is a non-Maxwellian two-temperature structure of the EPPC with the temperature of cold electrons, $T_{ec} = 0.73$ eV, and the temperature of hot electrons, $T_{eh} = 4.2$ eV; following Langmuir procedure yields the plasma density, $n_L = 5.9 \times 10^9$ cm^{-3}. The corresponding values after differentiation of the EPPC from the electron energy probability function (EEPF), $f(\varepsilon)$ shown in Fig. 4, are: $T_{ec} = 0.50$ eV and $T_{eh} = 3.4$ eV, with the effective electron temperature $T_{eff} = 2/3\langle\varepsilon\rangle = 0.67$ eV and plasma density $n = 4.4 \times 10^9$ cm^{-3}. In this case, the error of the plasma density calculated from the EPPC following Langmuir procedure is 34%.

In case of 0.3 Torr, this error becomes even more significant. The differences between the true plasma potential, V_s, at $d^2I_e(V)/dV^2 = 0$ and those found at the intersection point, V_{sL}, and at the inflection point, V_{si}, are shown in Fig. 3. The values of the electron saturation current I_{eo} found at V_{sL} and V_{si}, and calculated from these I_{eo} plasma densities, are lower than the true values of I_{e0} and n, by corresponding factors of 2.6 and 14.

The electron temperature found according to Langmuir procedure from the linear part of $\ln[I_e(V)]$ for 0.3 Torr (shown in Fig. 3), $T_{eL} = 1.37$ eV, while the effective electron temperature found from EEPF shown in Fig. 4 EEPF, $T_{eff} = 3.4$ eV, and $T_{eh} = 0.71$ eV. These numbers and those for 0.03 Torr demonstrate how misleading can be values of slow and fast electron temperatures found from the EPPC for non-Maxwellian plasmas following Langmuir routine.

The main reason for so large disparity in inferred values of the n and the T_e at 0.3 Torr is a non-Maxwellian, Druyvesteyn-like EEPF. This kind of distribution is typical in dc and rf discharges in Ramsauer gases (Ar, Kr, and Xe) at $\omega^2 \ll \nu_{en}^2$ and/or at relatively low plasma density when electron-electron collision frequency, $\nu_{ee} \sim nT_e^{-3/2}$, is not high enough to Maxwellize the electron energy distribution.

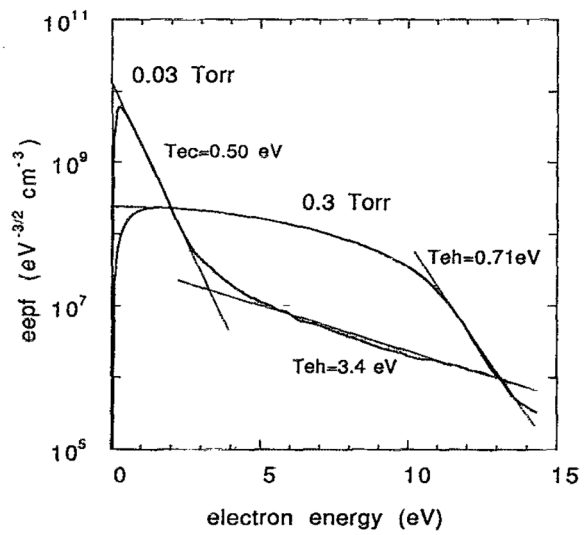

FIG. 4. EEPF for Ar CCP at 0.03 and 0.3 Torr obtained through double differentiation of the probe characteristics presented in Fig. 3.

Here, ω is the angular rf frequency, and ν_{en} is the electron-neutral collision frequency. A non-Maxwellian EEDF in both the elastic ($\varepsilon < \varepsilon^*$) and inelastic ($\varepsilon > \varepsilon^*$) energy ranges is typical for gas discharge plasmas. The EEDF in the elastic energy range may get close to the Maxwellian distribution (dependent on $\nu_{en}(\varepsilon)$ function, ω/ν_{en} ratio, and the plasma density), while in most cases, the EEDF in the inelastic energy range, $\varepsilon > \varepsilon^*$, visibly diverts from the EEDF in elastic energy range, $\varepsilon < \varepsilon^*$.

In the vicinity of the floating potential, V_f, only hot electrons ($\varepsilon \geq \varepsilon^*$) reach the probe, and the EPPC (inferred as $I_e = I_p - I_i$) gives extremely inaccurate presentation of the electron temperature of the hot electrons, T_{eh}, due to uncertainty in the ion current approximation (which is discussed later in this article).

When the plasma density is high (roughly, at $n > 10^{11}\,cm^{-3}$), the EEDF in the elastic energy range gets close to the Maxwellian distribution, and the plasma parameters found from the Langmuir routine and the EEDF do not differ significantly. However, the electron distribution temperature of fast electrons, T_{eh}, may be lower than T_{eL} (due to inelastic processes and lack of e-e collisions), or higher than T_{eL} (due to stochastic heating of fast electrons in low pressure capacitively coupled plasma, CCP and inductively coupled plasma, ICP).

In conclusion of this chapter, let us state main problems limiting application of the classic Langmuir probe diagnostics:

(a) Non-Maxwellian shape of EEDF in elastic energy range, $\varepsilon < \varepsilon^*$.
(b) Uncertainty in the plasma potential evaluation.
(c) Inaccuracy in finding T_{eh} due to arbitrariness of the ion current approximation.

These problems are intrinsic to the Langmuir procedure and they limit its applicability, although the experiment may comply with other important requirements of proper probe diagnostics, i.e., small probe size, absence of electron collisions, clean probe surface, no stray impedance in the probe circuit, and no rf and low frequency noise.[9] All three problems (a, b, c) mentioned above can be avoided by differentiation of the probe characteristic and obtaining the EEDF in wide range of electron energy.[7,10]

III. ION PART OF THE PROBE CHARACTERISTIC

The IPPC is frequently used for inferring the plasma density and temperature due to its simplicity. Unlike the EPPC, the IPPC acquisition does not require a large area reference (grounded) electrode to close the probe current path. The IPPC can be acquired in different arrangements, with a single, a double, or a triple probe. In all of these cases, the electron temperature, T_{ei}, is found from the IPPC in the vicinity of the floating potential, V_f. For a single probe

$$T_{ei} = eI_e[dI_e/dV]^{-1} = e(I_p - I_i)[dI_p/dV - dI_i/dV]^{-1}.$$

Usually, for a single probe, T_{ei} is found at the floating potential ($V = V_f$). It is advisable to choose the probe potential somewhat higher than V_f, which would minimize the impact of arbitrariness of the ion current approximation $I_i(V)$ on accuracy of T_{ei}; biasing beyond V_f can be applied to a single probe but not viable for floating double and triple probes.

The plasma density inferred from the IPPC, n_i, according to one of many ion current theories is found from the ion saturation current at a high negative potential. Two basic theories are used today for inferring the plasma density from the IPPC.[12] One of them, the radial motion theory (RMT), which accounts only for the radial ion motion to the probe, was proposed by Allen *et al.*[13] and modified by Chen[14] for the practical cylindrical probe. The RMT is also frequently referred to as ABRC theory, named after its authors. Another, the orbital motion theory (OMT), which accounts for the orbital ion motion, was proposed by Mott-Smith and Langmuir[15] (the OML theory), and later refined by Bernstein and Rabinowitz[16] and Laframboise.[17] The refined OMT is frequently referred to as BRL theory. Both, RMT and OMT assume absence of ion collisions in the orbital zone or/and the probe sheath area; they also assume a Maxwellian electron and ion energy distributions. There is no clear boundary between applicability areas of each theory. Applicability of the OMT usually implies $a_p/\lambda_D \ll 1$, while the RMT applicability usually suggests a final ratio $a_p/\lambda_D > 1$. Here, a_p is the probe radius, and λ_D is the electron Debye length.

While some publications affirm plausible agreement of the plasma densities, n_i found from the IPPC with the densities found from the EPPC and others independent diagnostics, special studies on this subject[10,18–21] point towards substantial differences between them. These studies demonstrated vast difference of n_i values found through OMT and RMT compared to the n calculated from the EPPC using the Langmuir procedure, the measured EEDF, and measurements with different microwave probe techniques.

For example, in Ref. 18, the plasma density found in the positive column of the dc discharge in helium at 40 mTorr and the discharge current 0.2 A, from the EEDF, from the orbital theory for electrons, the OMT, and the RMT for ions are, correspondingly, related as 1.0, 0.85, 9.0, and 0.25 (36 times difference in n_i values!). Similar patterns of significant differences between the plasma densities were found for helium and nitrogen over the range of discharge currents and gas pressures.[18]

Significant disagreements between plasma densities inferred from the ion OMT and the EEPF were found in a CCP at argon pressure 0.3 and 0.03 Torr.[10] The plasma density at $p = 0.03$ Torr found from the OMT was 2.5 times larger than from the EEPF, and for $p = 0.3$ Torr, was 3.3 times larger. On the other hand, calculation of the ion saturation currents according to the RMT[13,14] using plasma densities found from EEPF at 0.03 Torr showed 6.2 times larger current than found in the experiment.[10] This corresponds to underestimated plasma density inferred from the RMT in 6 times, similarly to that found in Ref. 18. The ion saturation current calculated according to the RMT for 0.3 Torr showed 0.72 of the measured current, although at $p = 0.3$ Torr the probe sheath is strongly collisional ($\lambda_i \ll d_s < R_0$) making both the RMT and OMT not applicable.

The ion current, I_{sim}, to a cylindrical probe in argon plasma at 1, 10, and 100 mTorr has been calculated by Iza

and Lee[19] using particle-in cell simulation. These gas pressures correspond to collisionless, weakly/moderate, and highly collisional ion motion in the probe vicinity. The simulations assumed a Maxwellian EEDF and fixed plasma density, n_0, and electron temperature.

Plasma densities calculated according to radial ABRC, orbital BRL, and Tichy *et al.*[20] (accounting for ion collisions) theories using the I_{sim} values have shown dramatic discrepancy with the plasma density n_0 set in the simulation. Thus, at 1, 10, and 100 mTorr, BRL theory, correspondingly, gave $n_i/n_0 \approx 3$, 4, and 2, while ABRC theory gave $n_i/n_0 \approx 0.3$, 0.45, and 0.14. Somewhat less disagreement was found in collisionless regime, and plausible agreement occurred in collisional regime using Tichy's theory[20] accounting for ion collisions: $n_i/n_0 \approx 2$, 0.75, and 0.9.

Comparison of plasma densities found from the EEDF measurement, cut-off and hairpin microwave probes, and from IPPC using OML theory has been performed in argon ICP between 7 and 22 mTorr.[21] Corresponding ratios for plasma densities were found as 1.0, 1.1, 1.45, and about 3; that, again, show considerable difference between the plasma density found from the ion part of the probe characteristic and those found from three others electrical and microwave probe methods.

Close values for plasma densities found from EEDF and cut-off probe (by measuring the plasma frequency, $\omega_{pe} = e(n/4\pi m)^{1/2}$) are not fortuitous, as both methods are based on theories with minimal assumptions. Indeed, both methods (within their applicability, i.e., when $a_p \ll \lambda_e$ and $\nu^2_{en} < \omega^2_{pe}$) do not depend on the probe geometry, EEDF, and electron and ion collision rate.

The results of above studies are presented in Table I, where the plasma densities, n obtained by different methods are related to those, n_0 found as appropriate integrals of the measured EEDFs. Plasma densities ratios, n/n_0 calculated according to OMT and RMT to those found in Ref. 19 through particle-in-cell simulation are also included in this table.

As seen from Table I, the plasma density values inferred from the IPPC using the OMT and RMT significantly diverge (often above an order of magnitude). Both IPPC and OMT data are consistently different from correspondent values obtained from EPPC and microwave probes (up to an order of magnitude). Ironically, some less discrepancy is observed for relatively high gas pressure when collisionless OMT and RMT are not applicable at all.

TABLE I. Plasma density error factor n/n_0.

Source	Gas/pressure	EPPC	Ion OMT	Ion RMT	Cut-off pr.	Hairpin pr.
Ref. 10	Ar, 30 mTorr	1.34	2.5	0.16		
Ref. 10	Ar, 0.3 Torr	0.38/0.07	3.3	1.4		
Ref. 18	He, 40 mTorr	0.85	9	0.25		
Ref. 21	Ar, 7–22 mTorr		2.6–3.25		1.1	1.5
Ref. 19	Ar, 1 mTorr		≈ 3	0.3		
Ref. 19	Ar, 10 mTorr		≈ 4	0.45		
Ref. 19	Ar, 0.1 Torr		≈ 2	0.14		

Table I shows plasma densities found from the EPPC in plausible agreement with those found with the cut-off probe and EEDF (except of argon CCP at $p = 0.3$ Torr, when the EEDF is strongly non-Maxwellian in the elastic energy range). In the last case, using the true plasma potential found through the EPPC differentiation results in even larger error (by the factor of 0.07). Apparently, the classical Langmuir procedure is not applicable for such plasmas.

Large diversion between the plasma density obtained from the IPPC and all others independent methods is attributed to many unrealistic assumptions put into IPPC theories. The most frequently mentioned reason for the discrepancy is ion-neutral collisions. Indeed, both the EPPC and the IPPC theories assume a collisionless motion of the charged particles in the area perturbed by the probe, in the space charged sheath and in the orbital zone; in abbreviated form this means $\lambda_i \gg d_s, R_o$, where λ_i is the ion mean free path, d_s is the probe sheath thickness, and R_o is the radius of the orbital zone.

Let us roughly estimate, what is the maximal gas pressure, p_{max}, at which the collisionless condition $\lambda_i \gg R_o$ is satisfied. For the cylindrical OMT, the radius of the orbital zone given in Ref. 22 is $R_o = a_p(-eV/T_i)^{1/2}$; thus, the absence of ion collisions is equivalent to $\lambda_i \gg a_p(eV/T_i)^{1/2}$, where T_i is the ion temperature. For the cylindrical RMT, i.e., for ABR/Chen theory at highly negative biased probe, the sheath thickness may be approximated as $d_s \approx 10\,\lambda_D$, and the collisionless condition is equivalent to $\lambda_i \gg 10\,\lambda_D$.

Assuming here and later, the sign "≫" staying for the factor of 10, and selecting typical plasma parameters $n = 1 \times 10^{11}$ cm^{-3}, $T_e = 3$ eV, $T_i = 0.03$ eV, the probe radius $a_p = 5 \times 10^{-3}$ cm, the ion mean free path for argon $\lambda_i = (p/300)$ cm, and the probe voltage $V = -60$ V, we obtain for applicability of OMT $p_{max} = 1.5$ mTorr, and for RMT = 7.4 mTorr. If $n = 1 \times 10^{10}$ cm^{-3}, RMT can be applied up to $p_{max} = 2.3$ mTorr. Such values of p_{max} correspond to the low end of the gas pressure range useful for the plasma processing and basic research applications.

For comparison, let us estimate p_{max} for applicability of the EPPC in Langmuir and Druyvesteyn procedures, which, correspondingly, involve $\ln[I_e(V)]$ and $d^2I_e(V)/dV^2$. The effect of electron-neutral collisions leads to depletion of the electron current to the probe at the vicinity of the plasma potential V_s where $d_s \approx \lambda_D$. This depletion at elevated gas pressure is caused by collisions in the probe sheath and presheath decreasing the electron diffusion to the probe.[9] The collisionless condition for applicability of the EPPC can be written as $\lambda_e \gg a_p + \lambda_D$. Taking the parameters values selected in the previous estimate and assuming for argon $\lambda_e = (1.5 \times 10^{-2}/p)$ cm, we find $p_{max} = 740$ mTorr. Thus, the maximal pressure where the EPPC can be applied is over two orders of magnitude larger than that for the IPPC. This seems a serious reason to be cautious when choosing the ion part of the probe characteristic for the plasma diagnostics.

There were many attempts to mend IPPC theories by accounting for ion collisions,[12,20–24] but they have not produce any reliable methods for practical applications. Obstacles in refining IPPC methods, to our mind, come from

the issues not addressed in IPPC original theories. Let us discuss these deficiencies.

As mentioned above, the electron temperature, specifically the electron energy distribution, EEDF is the key factor defining the shape of the IPPC. All IPPC theories make *a priori* assumption of a Maxwellian EEDF that is not the case for most of the gas discharge plasmas. The high-energy tail of the EEPF usually has its distribution temperature, T_{he}, different from the main body of electrons, T_{eL}; that is true even for very dense plasmas, where the main body of thermal electrons in the elastic energy range is Maxwellian. The tail distribution temperature, T_{eh}, can be lower than T_{eL}, due to electron inelastic collisions at $\varepsilon > \varepsilon^*$, or higher than T_{eL}, due to selective heating of high energy electrons as it occurs in the low pressure CCP[25] and ICP in the regime of the anomalous skin effect.[26]

Transition from T_{eL} to T_{he} in the gas discharge plasmas takes place around the transition energy, ε_{tr}, defined by the main processes of the EEPF tail depletion and enrichment, such as excitation, ionization, and electron escape to the wall balanced with electron heating and electron energy redistribution via e-e collisions. Except of the very low gas pressure, the transition energy, ε_{tr}, is close to ε^*, and this energy can be lower or higher than the energy corresponding to the probe floating potential, $-eV_f$. In IPPC routine, the electron temperature, T_{ei}, is defined at the floating potential, V_f, therefore, when $\varepsilon_{tr} < -eV_f$, T_{ei} is close to the bulk electron temperature, T_{eL}, and when $\varepsilon_{tr} > -eV_f$, T_{ei} is close to the tail electron temperature, T_{he}. Which case occurs in particular, experiment is not known in advance and can be found only after EEDF measurement.

Another source of uncertainty (subjected to the gas pressure variation) is the difference that was demonstrated above between values of T_{eL} and T_{he} found from the probe characteristic and those found from the EEPF. This leads us to conclusion that one cannot be sure of applying correct value of the electron temperature into IPPC routine unless knows *a priori* the real (rather than assumed) EEDF. The floating potential, V_f, is defined by the EEDF tail corresponding to electrons having high enough energy to reach the floating probe. If $T_{he} < T_{eL}$ (a depleted tail of the EEPF), $|V_f|$ is lower, while if $T_{he} > T_{eL}$ (an enhanced tail of the EEPF), $|V_f|$ is higher than the value predicted by using T_{eL}. It has been shown by Vasil'eva[27] that in the case of the non-Maxwellian EEDF, the plasma potential distribution in the presheath, the ion current to the probe, and the Debye length are defined neither by T_{eL} nor by the electron effective temperature, $T_{eff} = 2/3\langle\varepsilon\rangle$, but by the electron screening temperature, T_{es}

$$T_{es} = \left\{ 2\int_0^\infty \varepsilon^{-\frac{1}{2}} f(\varepsilon) d\varepsilon \right\}^{-1} \neq T_{eff} = \frac{2}{3}\int_0^\infty \varepsilon^{\frac{3}{2}} f(\varepsilon) d\varepsilon,$$

where $f(\varepsilon)$ is the EEPF.

Screening temperature, T_{es}, is weighted by low energy electrons, and, for shown in Fig. 4 EEPFs, T_{es} is close to $T_{ec} < T_{eff}$ for bi-Maxwellian EEPFs, while $T_{es} > T_{eff}$ for the Druyvestein-like distribution. In case of a Maxwellian EEDF, all electron temperatures are equal: $T_{es} = T_{eL} = T_{ec} = T_{he} = T_{eff} = T_e$. The departure from a Maxwellian EEDF could be accounted in IPPC theories by replacing T_e with T_{es}, but that cannot be done without *a priori* knowledge of the EEDF.

More effects are unaccounted for in the existing IPPC theories; these effects also may require additional assumptions about floating potential and the ion temperature. Let consider just few of them.

The ion ambipolar drift in the probe vicinity can make the probe ion current significantly different from its value calculated under no-drift assumption. In bounded gas discharge plasmas, the ion drift velocity v_i may considerably exceed the ion thermal velocity v_{iT}, in the discharge volume (but its center) since $v_{iT} \approx (T_i/M)^{1/2} < v_i \leq v_s = (T_{es}/M)^{1/2}$. Although there are theories to account for the unidirectional ion motion in plasma,[4] we are not aware of applying them to IPPC analyses of gas discharge plasmas. In any case, that would require further assumptions about the ambipolar field value and its direction reference to the probe orientation.

The deformation of the probe sheath or the orbital zone from cylindrical to ellipsoidal may significantly distort the ion motion around the probe, thus affecting the ion current to the probe; such deformation takes place at high negative probe potential, low plasma density, and small ion temperature.

According to OMT theory, the ion current dependence is $I_i(V) \sim V^{1/2}$ for a cylindrical orbital zone and $I_i(V) \sim V$ for a spherical zone. The orbital zone approaches a spherical shape when its size becomes comparable to the probe half-length, $l/2$. For typical plasma parameters and the probe radius, considered above ($n = 10^{11}\,cm^{-3}$, $T_e = 3\,eV$, $T_i = 0.03\,eV$, $a_p = 5 \times 10^{-3}\,cm$), the orbital zone radius, $R_0 = 1.7\,mm$, is comparable with $l/2$ of a practical probe length, $l = (3\text{–}10)\,mm$. Since the radius of the cylindrical orbital zone, R_0, is proportional to the probe radius, a_p, for frequently used in experiments probe radii larger than $5 \times 10^{-3}\,cm$, one would expect the validity of spherical, rather than cylindrical OMT.

Similar effect would show up at the radial ion motion at low plasma density and large negative probe potential, when the probe sheath thickness $d_s \approx 10\,\lambda_D$ is comparable to $l/2$. Not taking these deformations into account is a serious drawback in applying present IPPC theories to real experiments. We believe that mentioned above effect non-accounted in IPPC theories are the reason for notorious inaccuracy in the plasma parameters inferred from these theories.

We doubt "surprising validity of OML theory,"[12] based on the fact that the ion current to the cylindrical probe can be well fitted to $I_i(V) \propto V^{1/2}$ dependence by varying two unknown values: the plasma potential and the plasma density. This validity has not been proven with independent plasma density measurements in the same plasma. The dependence $I_i(V) \propto V^{1/2}$ is not a sufficient condition to ensure validity of OML theory.

Our understanding is that none of the existing theories for the ion part of the probe current can consistently yield accurate plasma parameters and make dependable tools for plasma diagnostics. An exception could be the RMT applied to a very dense plasma when $\lambda_D < a_p \ll \lambda_i$, with a Maxwellian EEDF up to the electron energy well exceeding the floating probe potential; but the very existence of such

condition has to be confirmed by EEDF measurements or established through a strong theoretical argument.

For example, let us consider dense plasma with cold electrons when the frequency of the electron-electron collisions, $\nu_{ee} \propto nT_e^{-3/2}$, is large enough for EEDF Maxwellization. In this case, the EEDF can be Maxwellian up to the electron energy ε within the interval $|eV_f| < \varepsilon < \varepsilon^*$ for all electrons participating in formation of the probe characteristic around the probe floating potential. In argon plasma $\varepsilon^* = 11.56\,eV$, and a Maxwellian EEDF around V_f is possible in a weak electron heating electric field, with $T_e < (1–2)$ eV and $|eV_f| < (4–8)$ eV.

Applying traditional techniques, which use the EPPC and the IPPC for processing of the probe characteristic obtained in the non-equilibrium plasma, may lead to significant errors (up to an order of magnitude) in calculating the plasma basic parameters. The accuracy especially deteriorates when the inferred value of T_{ei} found at the floating potential, V_f, and represents only a small portion of electrons of the high-energy tail of the EEDF. Departure of high-energy electrons from Maxwellian distribution is quite common in low-pressure gas discharge plasmas, while the extent of this departure is not known in advance. Therefore, acquisition of the full probe characteristic followed by its differentiation (to get EEDF) is the most informative and reliable way of the plasma probe diagnostics.

IV. EEDF MEASUREMENTS

The electron velocity distribution function (EVDF), $\mathbf{F_v}(\mathbf{r},\mathbf{v},t)$, is the most complete characteristic of plasma electrons. Here, **r** and **v** are coordinate and velocity vectors. Having the EVDF, one can find the plasma basic parameters, transport, and chemical reaction coefficients as corresponding integrals of the EVDF. Usually, except the case when the ratio of the electric field to the gas density, E/N, is very high, electrons in the bounded gas discharge plasma exhibit relatively small anisotropy, and their energy distribution can be quite accurately represented by the sum of an isotropic EVDF, $F_{v0}(\mathbf{r},v,t)$, and a small anisotropic part, $\mathbf{F}_{v1}(\mathbf{r},v,t)$. For practical purposes, since $F_{v0} \gg |\mathbf{F}_{v1}|$, the plasma parameters, electron transport, and reaction coefficients are defined only by $F_{v0}(\mathbf{r},v,t)$ or by the EEDF, $F_e(\mathbf{r},\varepsilon,t)$.

Druyvestein[28] has shown that in isotropic plasmas the EEDF can be found by differentiation of the probe characteristic according to

$$\frac{d^2I_e}{dV^2} = \frac{e^2S_p}{4}\sqrt{\frac{2e}{mV}}F_e(\varepsilon) = \frac{e^2S_p}{2\sqrt{2}}f(\varepsilon),$$

where $f(\varepsilon) = \varepsilon^{-1/2}F_e(\varepsilon)$ is the EEPF that for the Maxwellian distribution presents a straight line on a semi-log scale. The plasma density and effective electron temperature for an arbitrarily shaped EEPF can be calculated as

$$n = \int_0^\infty \sqrt{\varepsilon} f(\varepsilon)d\varepsilon \quad \text{and} \quad T_{eff} = \frac{2}{3}n^{-1}\int_0^\infty \varepsilon^{\frac{3}{2}} f(\varepsilon)d\varepsilon.$$

Still, making accurate measurements and differentiation of the probe characteristic turned out not a trivial task. It took over three decades after Druyvestein published his formula to demonstrate first experimental results and two more decades to make EEDF measurements a standard procedure.

The fundamental limitation of EEDF measurements comes from the noise generated in the gas discharge plasma and noise augmentation inherent to the differentiation procedure. The accuracy of the EEDF can be judged by the sufficient energy resolution ($\delta\varepsilon \le 0.3\ T_e$) and sufficiently wide dynamic range required to detect fast electrons (3–4 orders of magnitude).[7,9] Instruments meeting such requirements should make the most out of the high-end analog electronics and digital processing.

The fundamentals of EEDF measurements and various techniques for differentiation, smoothing, and processing of the probe I/V characteristics, as well as the analysis of distortions in EEDF measurements and remedies for their mitigation, can be found in reviews[7,9] and in the references given in those publications.

Comprehensive studies of EEDFs in capacitive[29] and inductive discharges[30] that revealed some new electron kinetics effects[31–34] have been performed in argon rf plasmas with a real-time display of the EEPF and the plasma basic parameters, T_{eff} and n. The examples of measurements of EEDFs in argon CCP[29] and ICP[30] in a wide range of gas pressure are shown, correspondingly, in Figs. 5 and 6.

The real-time display ($t = 0.1–1$ s) of the probe characteristic derivative, $d^2I_p/dV^2 \sim f(\varepsilon)$, is the unique way to detect problems in the probe measurements associated with the probe contamination, distortions by the low and rf frequency noise, a stray impedance in the probe circuit, and

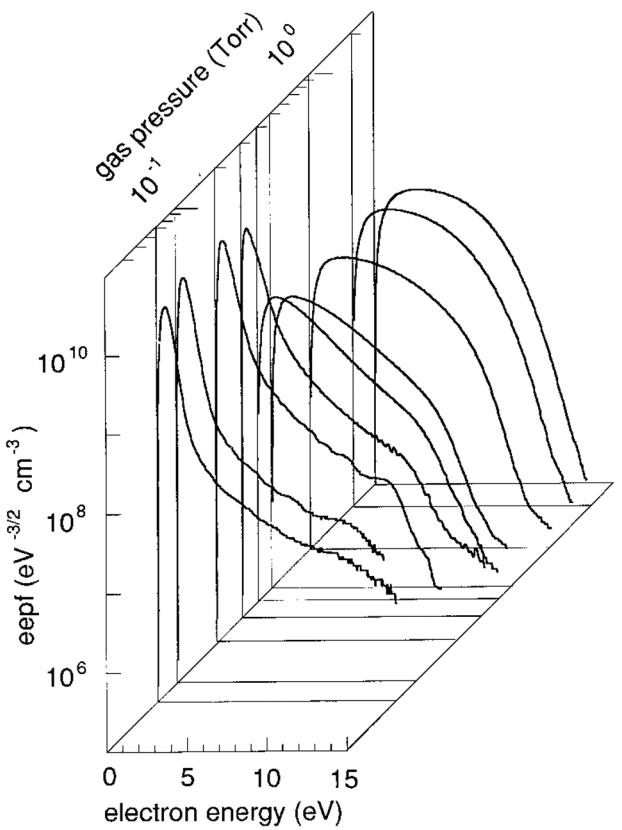

FIG. 5. EEPF in CCP at 13.56 MHz at different argon pressure.[29]

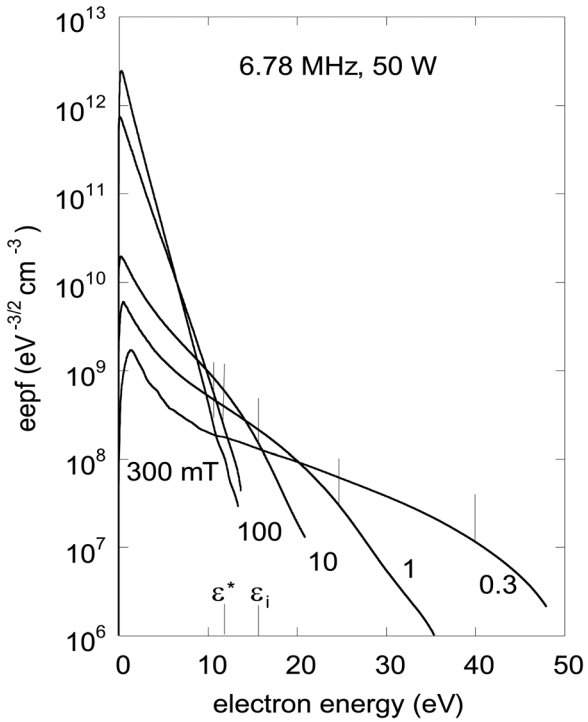

FIG. 6. EEPF in ICP at different argon pressure.[30] Vertical lines show plasma potentials.

others.[9] Differentiation of the probe characteristic also opens unique possibility for momentary acquisition of the precise plasma potential and the distribution of fast electrons in the inelastic energy range.

While basic research experiments are usually design to facilitate the probe diagnostics, making accurate measurements in the plasma processing reactors requires getting over many convoluted problems. Large rf plasma potentials at the fundamental frequency and its several harmonics, low-frequency noise due to ionization instabilities in molecular and electronegative gases, the probe surface, and the chamber wall contamination by low-conductive deposits lead to significant distortions of the probe characteristics. These distortions are hard to recognize on the probe I/V characteristic, they become apparent only on its derivatives. Importance of the real-time display of the second derivative is often ignored, and many publications show significantly distorted EEPFs measured with some commercial or in-house assembled probe systems. Such EEPFs are usually missing information about low energy ($\varepsilon \lesssim T_e$) and high-energy ($\varepsilon \gtrsim \varepsilon^*$) electrons. Examples of such measurements are discussed below.

V. ESSENTIAL FEATURES OF THE PROBE SYSTEMS FOR EEDF MEASUREMENTS

Building in-house probe system for reliable EEDF measurement is not a trivial task. Lately, many researchers making probe measurements have turned to commercial instruments. These probe systems are built by different companies in different countries and claim advantages of their instruments over competitor's. Sometimes, such claims have very little to do with actual capability of the instruments to deliver accurate results.

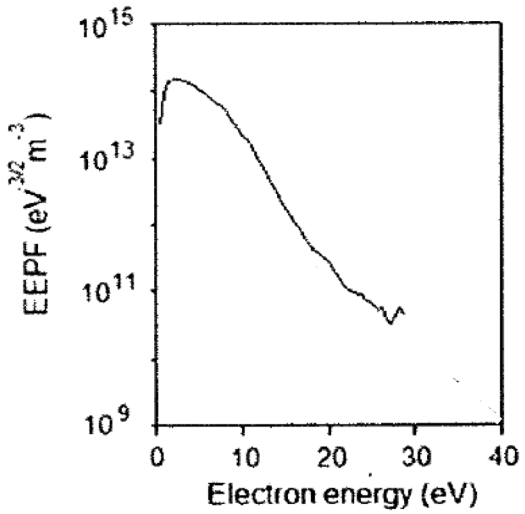

FIG. 7. EEPF in ICP at argon pressure of 2.2 mTorr.[39]

Since no standardized tests or any unified specifications have been developed for the plasma probe instruments, their performance can only be assessed by available measurement results. We put together the results of EEPF measurements in similar plasmas measured in different laboratories with different probe systems.[35–38] These results are presented in Figs. 7–11.

EEPFs measured with different instruments in argon ICPs at similar conditions are shown in Figs. 7–9. The shape of EEPF[39] measured with the instrument[35] and shown in Fig. 7 is convex in its low energy part resembling a Druyvestein distribution. Very different EEDFs shapes[40] are obtained in the similar plasma measured with two others probe systems[37,38] and shown in Fig. 8. Here, both measured EEPFs are very similar to each other and demonstrate concave shapes in the low energy part of EEPFs, while showing different energy resolution and level of noise.

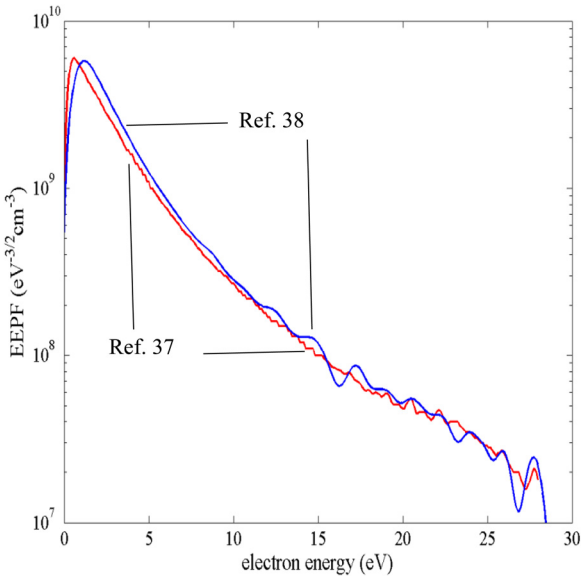

FIG. 8. EEPFs in ferromagnetic enhanced ICP in argon at 1.2 mTorr (Ref. 40) measured with different probe systems.[37,38]

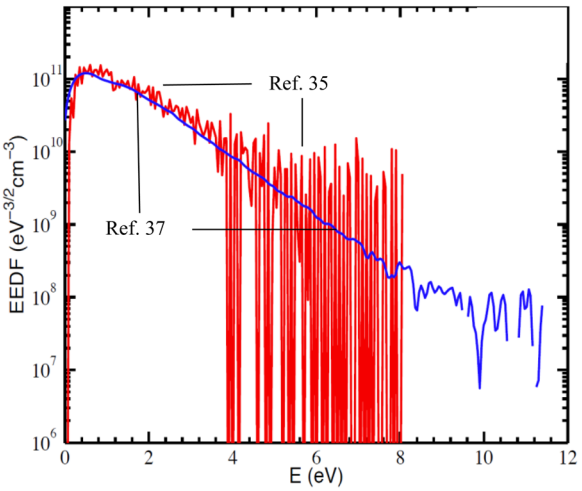

FIG. 9. EEPFs measured in PEGASUSE propulsion system[41] with different probe instruments.[35,37] Note the both EEPFs are distorted (deviate from Maxwellian) in the low energy range. The reason is the absence of the stray impedance compensation feature in the used home-made probe.

The energy resolution is an essential parameter affecting the accuracy of the EEDF measurement, and it is defined by the energy interval, $\Delta\varepsilon$, between the zero crossing and the maximum of the EEPF.[7,9] High energy resolution requires fast response time, competing with other instrument design requirements, such as plasma noise suppression and acquisition rate of the full EEDF. The interval, $\Delta\varepsilon$, is also increased by the probe contamination, stray impedance in the probe current path, and the plasma potential instability.[9] The criterion for acceptable energy resolution is $\Delta\varepsilon < T_e$, otherwise the information about low energy electrons is lost, while those electrons are the bulk of the plasma density. High accuracy in measured EEPF requires $\Delta\varepsilon/T_{eL} \leq (0.3–0.5)$. The EEDFs shown in Fig. 8 have the temperature of the low energy group, $T_{el} \approx 2.0$ eV, but different energy resolution, $\Delta\varepsilon/T_e = 0.25$ and 0.62.

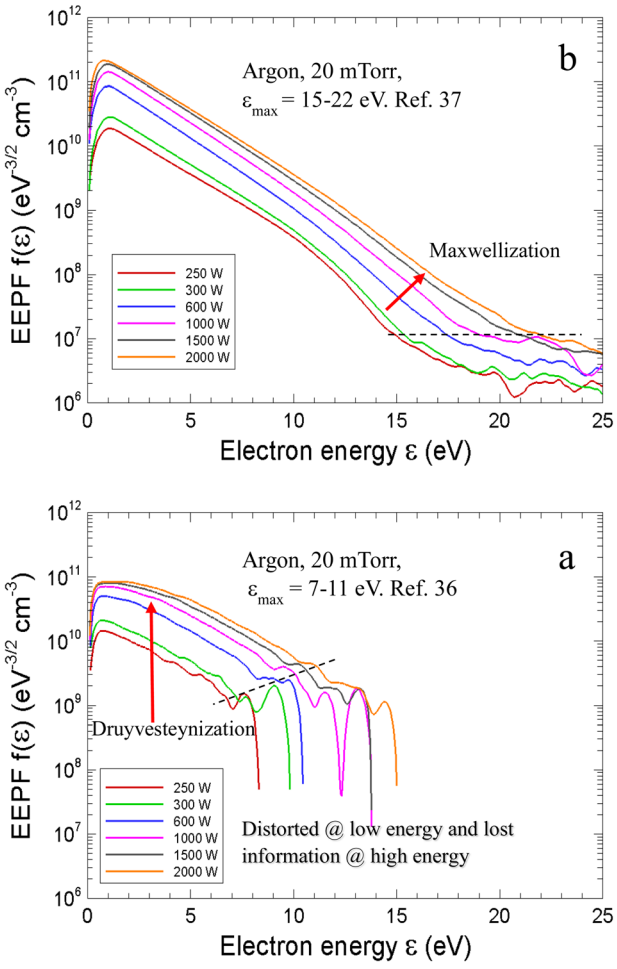

FIG. 10. EEPFs measured with different probe systems[36,37] in the same plasma.[9] Dashed lines indicate the noise threshold limiting reliable EEPF measurement.

The EEDFs with low energy peak (similar to that shown in Fig. 8) at very low gas pressure are common in the CCP dominated by the sheath heating (Fig. 5) and in the ICP in the regime of anomalous skin effect (Fig. 6). The EEDF of the similar plasma shown in Fig. 7 is apparently distorted, likely, by the "Druyvesteinization" effect[9] caused by the stray impedance in the probe measurement circuit. The stray impedance compensation is an important function of the EEDF instrument and was implemented in probe system to obtain undistorted EEDFs shown in Figs. 5 and 6.

Another important characteristic of the EEPF measurement instrument is its dynamic range that is the ratio between the EEPF maximum and its minimal values undistorted by noise. The dynamic range of a probe system limited by noise defines the system ability to get the high-energy part of the distribution undistorted. A desirable dynamic range for EEPF measurements is about 3–4 orders of magnitude, which corresponds to the confident energy interval $\varepsilon_{max} \approx (7–9)T_e$ for a Maxwellian EEDF. Larger dynamic range in the measured EEPF may be affected by the second derivative of the ion current.[9]

The confident energy intervals measured in the noisy plasma[41] with two probe systems[35,36] are demonstrated in Fig. 9, where $\varepsilon_{max} \approx 4$ eV (corresponding to dynamic range of 10) is found for one system, while $\varepsilon_{max} \approx 10$ eV (corresponding to the dynamic range of 10^3) is found for other system.

The dynamic range is, obviously, a problem for the data obtained in the plasma processing reactor with argon at varying rf power,[9] as shown in Fig. 10(a). In this case, the confidence energy interval, ε_{max}, is only a half of that shown in Fig. 10(b) demonstrating the dynamic range of 3–4 orders of magnitude. Similar measurements in the same reactor with oxygen plasma presented in Fig. 11(a) show ε_{max} even further skewed by the plasma noise, which can be suppressed as demonstrated in Fig. 11(b).

Difficulties in getting accurate EEPF measurements in processing reactors operating with complicated gas mixture of molecular and electro-negative gases are compounded by significant level of multi-frequency rf and low frequency noise and deposition of low-conductive films on the probe surface and chamber wall. Such conditions require the probe filters with extra high rf rejection, sophisticated algorithms for the low-frequency noise suppression, automated probe cleaning routines, and mitigation of the stray impedance of the probe circuit.

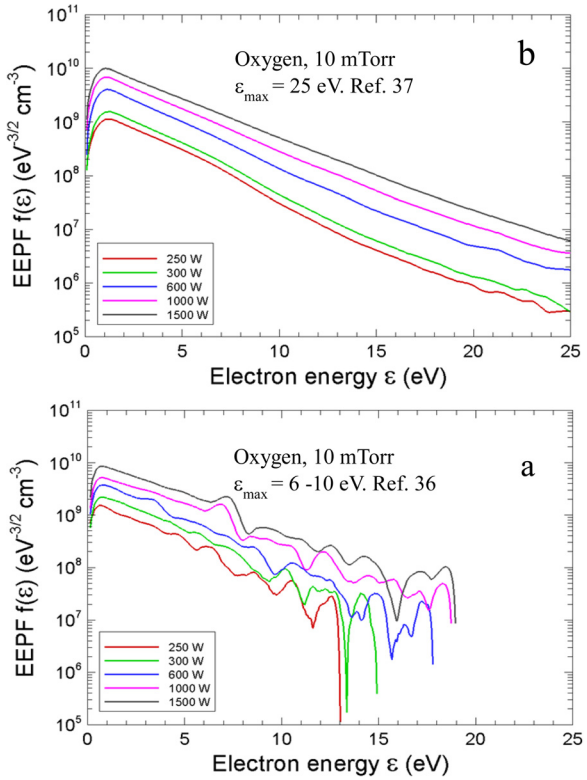

FIG. 11. EEPFs measured with different probe systems in the same (as in Fig. 10) ICP reactor with oxygen.

A detailed comparison of EEPFs measured with different probe systems in an ICP plasma reactor shown in Figs. 10 and 11 reveals more about their significant differences.[9] As seen in Fig. 10(b), the low energy ($\varepsilon < \varepsilon^*$) part of EEPFs for rf power ranging from 0.25 to 2 kW is Maxwellian. At low power, the EEPF slope changes at energy $\varepsilon > \varepsilon^* = 11.56$ eV, which is clearly visible for P = 250 W, indicating depletion of energetic electrons in the inelastic energy range. Increasing rf power gives rise to the plasma density and, thus, to electron-electron collision frequency which leads to Maxwellization of the EEPF tail. At 2.0 kW ($T_e = 2.2$ eV and $n = 1 \times 10^{12}$ cm^{-3}), the EEDF becomes very close to Maxwellian even above argon ionization energy, $\varepsilon^i = 15.76$ eV. None of these details are distinguishable in Fig. 10(a).

The data presented in Fig. 10(a) show evolution of EEDF from Maxwellian at low power to Druyvestein-like at high rf power. Such "de-Maxwellization" of EEDF when the plasma density is increasing contradicts to plasma physics, it points up to a deficiency of the instrument, most likely, its failure to compensate stray resistance of the probe circuit. The data obtained with the same instrument in oxygen discharge, see Fig. 11(a), look Maxwellian-like in the energy range below 6 eV at all powers. This "improvement" is due to the fact that the plasma density in oxygen ICP is substantially smaller than in argon for the same power. That makes the probe current significantly smaller and reduces EEDF distortions inflicted by the uncompensated stray resistance of the probe current path.

EEDF measurements in chemically active processing plasmas may present serious challenge due to rapid probe contamination. The probe coating affecting measurements

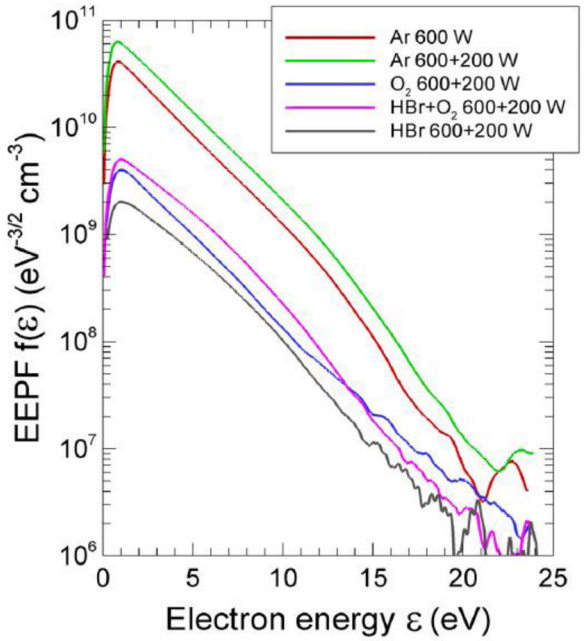

FIG. 12. EEPFs measured with[37] in an industrial ICP reactor filled with different processing gases: Ar, O_2, HBr+O_2, and HBr at 15 mTorr.[42]

may occur in less than few milliseconds, and the probe cleaning before measurements may not be enough. The good news is that probes may be cleaned in intervals between successive data acquisitions. The choice and effectiveness of a particular cleaning algorithm depend on the actual deposition rate and may require a bit of experimentation while looking at the real-time EEPF display. Monitoring the probe characteristics and its derivatives makes possible immediate recognition of distortions.

Different techniques for mitigating problems mentioned above[9] give opportunities for high quality EEDF measurements in harsh environment of plasma processing reactors. Examples of such measurements are given Figs. 12–14.

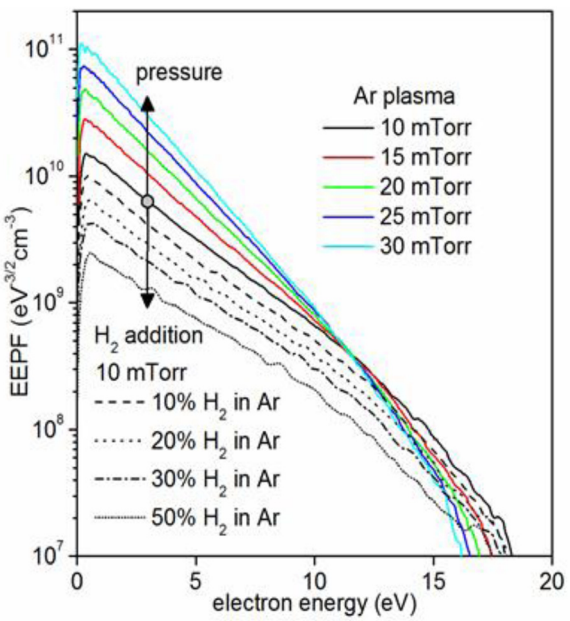

FIG. 13. EEPFs measured with[37] in ICP filled with Ar+H_2.[43]

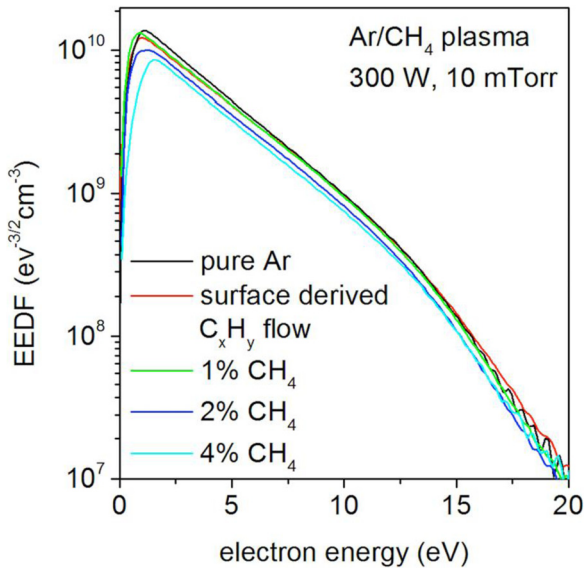

FIG. 14. EEPFs measured with[37] in ICP filled with Ar+CH_4 at the condition of strong polymer film deposition.[44] The deviation from Maxwellian EEPFs is clearly seen at $\varepsilon > \varepsilon^* = 11.56\,\text{eV}$.

Fig. 12 demonstrates EEPFs measured in a two-inductor ICP reactor,[42] operated with Ar, O_2, HBr, and HBr+O_2 at 15 mTorr. While argon data demonstrate the baseline quality of the measurements, small $\Delta\varepsilon/T_e$ values and high dynamic range of EEDFs in the reactive gas environment give confidence in these data.

Similarly trustworthy EEPFs are shown in Fig. 13, they were measured in ICP reactor operating in pure Ar gas and Ar + H_2 mixture.[43] The energy resolution, $\Delta\varepsilon/T_e \approx 0.1$, and the dynamic range of 3–4 orders of magnitude are evidences of good EEPF accuracy. Such data can be used with full confidence for plasma density, electron temperature, and reaction rate calculations as appropriated integrals of EEDF.[43]

The EEPFs measured in the same reactor operating with Ar and CH_4 added to plasma from surface and gaseous sources[44] are shown in Fig. 14. Despite intense polymer film deposition in this reactor, the measured EEPFs demonstrate good energy resolution, high dynamic range, and low noise level.

VI. CONCLUDING REMARKS

Ubiquitous Langmuir probe diagnostics is the subject of inaccuracies associated with non-Maxwellian electron energy distribution, uncertainty in locating the plasma potential, and arbitrariness in the ion current extrapolation. These shortcomings may lead to significant errors in the inferred plasma parameters, n and T_e. The errors in T_e and n mainly occur because of diversion of the EEDF from the Maxwellian distribution in the elastic energy range. In such cases, the traditional Langmuir procedure is not applicable for accurate measurement of plasma parameters.

The error in locating the plasma potential gets exponentially augmented in inference of the plasma density value. The error due to arbitrariness in the ion current extrapolation creates uncertainty in $I_e(V)$ at $V < V_f$, that becomes pronounced in low-density plasmas with rising of λ_D/a_p ratio.

Numerous studies comparing the plasma density found from the IPPC and EPPC (using Langmuir and Druyvestein procedure), as well as from different microwave probes, have demonstrated differences up to an order of magnitude. Comparison of plasma densities obtained with ion orbital and radial motion theories shows even more diversion.

Such significant differences in plasma parameters are due to deficiencies in existing IPPC theories making numerous assumptions, which are not always valid for real plasma conditions. The most detrimental of them is the assumption of a Maxwellian EEDF, although ion collisions and distortion of one-dimensional structure around cylindrical probe and ambipolar field unaccounted in existing IPPC theories can be essential problems.

A non-Maxwellian EEDF can be incorporated into existing IPPC theories, but this requires *a priori* knowledge of the EEDF. The IPPC collisionless theories cover only the gas pressure range up to few mTorr, while collisionless requirements of Langmuir and Druyvestein theories for the EPPC are valid (depending on probe size) up to fraction and few Torr.

Based on comprehensive studies in Refs. 10, 18, 19, and 21, we conclude that the plasma density inferred from the ion part of the probe characteristic consistently differs from other methods. That makes plasma parameters inferred from IPPC with a thin cylindrical probe unreliable.

Demand in past decades for development of the low gas pressure, technological plasmas fueled further progress of the gas discharge physics. It evolved from the local fluid paradigm to non-local kinetic paradigm involving phenomena of non-local and non-linear electrodynamics.[45–51] Non-equilibrium plasmas created by dc and rf fields at low gas pressure are rarely Maxwellian (even in the elastic energy range), and the only meaningful way for their diagnostics with Langmuir probe is high resolution measurement of an actual, non-Maxwellian EEDF over wide energy span. Accurately measured electron energy distribution allows unambiguous calculation of the plasma parameters and rates of the transport and reaction processes as corresponding integrals of the measured EEDF.

The collisionless probe theory for the electron part of the probe characteristic used in Langmuir and Druyvestein methods, as well as the concept of the cut-off probe, is founded on well-defined basic principles, giving these methods definite advantage over alternatives. Few limitations of these methods are unambiguous and have proven practical solutions to comply.[7–9]

Taking the derivatives, dI/dV and/or dI^2/dV^2 of the probe characteristics is the credible way for pinpointing the plasma potential, while the real-time display of the I(V) derivatives makes possible detection and mitigation of problems which may occur in a particular measurement setup.

Reviews[7,9] set guidelines for quality of EEDF measurements and described in details different methods to accomplish them. These reviews also discuss numerous problems and practical approaches to overcome them in order to make accurate measurements. However, many published results of EEDFs obtained with commercial or in-house assembled

probe systems do not suffice requirements of the state-of-the-art plasma science and technology.

Numerical simulation codes are now the main tool for analyzing the plasma electrodynamics, transport, and kinetics in commercial reactors. Simulation codes applied to complex processing gases are sometimes lacking reliable plasma-chemical cross sections; they also ignore effects of nonlocal and nonlinear plasma electrodynamics which is dominant in rf plasmas at low gas pressure. It is essential to validate numerical codes by comparing their prediction with actual plasma parameters obtained from measured EEDF.

Examples of high quality EEDFs measurements are presented in Figs. 10–14. These measurements performed in harsh conditions of commercial plasma reactors with chemically active mixtures prove their feasibility, providing adequate instruments and basic probe handling skills.

ACKNOWLEDGMENTS

This work was partially supported by the DOE OFES (Contract No. DE-SC0001939). The authors are thankful to A. Aanesland, Y.-K. Poo, and V. Nagorny for sharing with us the results of their measurements.

[1]I. Langmuir and H. M. Mott-Smith, Gen. Electr. Rev. **27**, 449, 538, 616, 762, 810 (1924).
[2]F. F. Chen, in *Plasma Diagnostic Techniques*, edited by R. H. Huddlestone and S. L. Leonard (Academic, NY, 1965).
[3]J. D. Swift and M. J. R. Schwar, *Electrical Probes for Plasma Diagnostics* (Iliffe Books, London, 1970).
[4]P. M. Chung, L. Talbot, and K. J. Touryan, *Electric Probes in Stationary and Flowing Plasmas: Theory and Application* (Springer, Berlin, Heidelberg, New York, 1975).
[5]B. E. Cherrington, Plasma Chem. Plasma Process. **2**, 113 (1982).
[6]N. Hershkowitz, *Plasma Diagnostics* (Academic, Boston, 1989), Vol. 1.
[7]V. A. Godyak, *Plasma–Surface Interaction and Processing of Materials* (Kluwer, Deventer, 1990).
[8]V. I. Demidov, S. V. Ratynskaia, and K. Rypdal, Rev. Sci. Instrum. **73**, 3409 (2002).
[9]V. A. Godyak and V. I. Demidov, J. Phys. D: Appl. Phys. **44**, 233001 (2011).
[10]V. A. Godyak, R. B. Piejak, and B. M. Alexandrovich, J. Appl. Phys. **73**, 3657 (1993).
[11]L. Schott, in *Plasma Diagnostics*, edited by W. Lochte-Holtgreven (North-Holland/Wiley, Amsterdam/New York, 1968).
[12]F. F. Chen, Plasma Sources Sci. Technol. **18**, 035012 (2009).
[13]J. E. Allen, R. L. F. Boyd, and P. Reynolds, Proc. Phys. Soc. B **70**, 297 (1957).
[14]F. F. Chen, *Modern Uses of Langmuir Probes* (Institute of Plasma Physics, Nagoya, Japan, 1985), Rept. IPPJ-750.
[15]H. Mott-Smith and I. Langmuir, Phys. Rev. **28**, 727 (1926).
[16]I. B. Bernstein and I. N. Rabinowitz, Phys. Fluids **2**, 112 (1959).
[17]J. G. Laframboise, University of Toronto Institute of Aerospace Studies, Report No. 100 (1966).
[18]I. D. Sudit and R. C. Woods, J. Appl. Phys. **76**, 4488 (1994).
[19]F. Iza and J. K. Lee, J. Vac. Sci. Technol., A **24**, 1366 (2006).
[20]M. Tichy, M. Sicha, P. David, and T. David, Contrib. Plasma Phys. **34**, 59 (1994).
[21]W.-K. Kim, M.-H. Lee, and C.-W. Chung, J. Korean Phys. Soc. **40**, 1687 (2006).
[22]C. H. Shih and E. Levi, AIAA J. **9**, 1673 (1971).
[23]Z. Sternovsky, S. Robertson, and M. Lampe, J. Appl. Phys. **94**, 1374 (2003).
[24]J. L. Jauberteau and I. Jauberteau, Plasma Sources Sci. Technol. **17**, 015019 (2008).
[25]V. A. Godyak and R. B. Piejak, Phys. Rev. Lett. **65**, 996 (1990).
[26]V. A. Godyak and V. I. Kolobov, Phys. Rev. Lett. **81**, 369 (1998).
[27]I. A. Vasil'eva, High Temp. **12**, 409 (1974).
[28]M. J. Druyvestein, Z. Phys. **64**, 781 (1930).
[29]V. Godyak, R. Piejak, and B. Alexandrovich, Plasma Sources Sci. Technol. **1**, 36 (1992).
[30]V. Godyak, R. Piejak, and B. Alexandrovich, Plasma Sources Sci. Technol. **11**, 525 (2002).
[31]V. Godyak, in *Electron Kinetics and Application of Glow Discharges*, edited by U. Kortshagen and L. D. Tsendin (Plenum Press, New York, 1998), pp. 241–255.
[32]V. Godyak, R. Piejak, and B. Alexandrovich, Phys. Rev. Lett. **68**, 40 (1992).
[33]V. Godyak, R. Piejak, and B. Alexandrovich, in *Proceedings of the 9th International Symposium on the Science and Technology of Light Sources*, edited by R. S. Bergman (Cornel University, Ithaca, NY, 2001). p.157.
[34]V. Godyak, B. Alexandrovich, and V. Kolobov, Phys. Rev. E **64**, 026406 (2001).
[35]See www.impedans.com for Langmuir Probe.
[36]See www.hidenanalytical.com, ESPion system.
[37]See www.plasmasensors.com for Plasma Diagnostics.
[38]See www.plasmart.com for DLP 2000 (discontinued).
[39]D. Gahan, B. Dolinaj, and M. B. Hopkins, Plasma Sources Sci. Technol. **17**, 035026 (2008).
[40]Y. K. Poo, private communication (2014).
[41]A. Aanesland, private communication (2014).
[42]V. Nagorny and D.-S. Lee, presented at ISPC, Philadelphia (2011).
[43]N. Fox-Lyon *et al.*, J. Phys. D: Appl. Phys. **46**, 485202 (2013).
[44]N. Fox-Lyon *et al.*, J. Vac. Sci Technol., A **32**, 030601 (2014).
[45]V. Kolobov and V. Godyak, IEEE Trans. Plasma Sci. **23**, 503 (1995).
[46]L. D. Tsendin, Plasma Sources Sci. Technol. **4**, 200 (1995).
[47]U. Kortshagen, C. Bush, and L. D. Tsendin, Plasma Sources Sci. Technol. **5**, 1 (1996).
[48]M. Lieberman and V. Godyak, IEEE Trans. Plasma Sci. **26**, 955 (1998).
[49]V. Godyak, Phys. Plasmas **12**, 3553 (2005).
[50]V. Godyak, IEEE Trans. Plasma Sci. **34**, 755 (2006).
[51]L. D. Tsendin, Phys. - Usp. **53**(2), 133 (2010).